

1 Experimental assessment of different mixing air ventilation 2 systems on ventilation performance and exposure to exhaled 3 contaminants in hospital rooms 4

5 F.A. Berlanga^{a1}, I. Olmedo^a, M. Ruiz de Adana^a, J.M. Villafruela^b, J.F. San José^b, F. Castro^b

6 ^aDepartment of Chemical Physics and Applied Thermodynamics, University of Córdoba, 14014 Córdoba, Spain

7 ^bDepartment of Energy and Fluid Mechanics, University of Valladolid, 47011 Valladolid, Spain

8 felix.berlanga@uco.es

9

10 **Nomenclature**

ACH	Air changes per hour (h^{-1})
AIIR	Airborne infection isolation room
CFD	Computational fluid mechanics
CP	Patient
D	Exhaust grille placed on the lower part of the West wall
DR	Percentage of dissatisfied people as a result of draught
DV	Displacement ventilation
G	Supply grille diffuser placed on the East wall of the room
GD	Ventilation system configuration combining G supply and D exhaust
GU	Ventilation system configuration combining G supply and U exhaust
IHR	Individual hospital room
IF	Intake fraction
IF_{max}	Maximum intake fraction
$IF_{125\%}$	Peaks average intake fraction
S	Supply swirl diffuser placed on the ceiling of the room
SD	Ventilation system configuration combining S supply and D exhaust
SU	Ventilation system configuration combining S supply and U exhaust
U	Exhaust grille placed on the upper part of the West wall
$\langle \bar{c} \rangle$	Mean tracer gas concentration of contaminant of the chamber (ppm)
\bar{c}_e	Average tracer gas concentration of the exhaust air (ppm)
\bar{c}_p	Average tracer gas concentration in a determined point (ppm)
$\bar{c}_{P,125\%}$	Average peaks tracer gas concentration in a determined point (ppm)
$c_{p,max}$	Maximum tracer gas concentration in a determined pint (ppm)
$\bar{c}_{CP,exh}$	Average contaminant concentration emitted through the CP exhalation (ppm)
\bar{c}_s	Average tracer gas concentration in the supply air (ppm)
e_p^c	Local relative exposure coefficient
$e_{P,125\%}^c$	Local relative average peaks concentration exposure coefficient
$e_{p,max}^c$	Local relative maximum exposure coefficient
$f_{P,125\%}$	Local maximum exposure frequency (h^{-1})
H	Total height of the chamber (m)

HR_i	Average relative humidity in a determined point (%)
HW	Health worker
IAQ	Indoor air quality
IF	Intake fraction
Inh	Point located inside the inhalation airway of HW manikin
MV	Mixing ventilation
P3	Pole located far from thermal loads
PHW	Pole located near health worker location
PCP	Pole located near patient location
PMV	Predicted mean vote
PPD	Predicted percentage of dissatisfied (%)
ppm	Particles per million
$Q_{b,exh}$	Exhaled volume of CP (l/min)
$Q_{b,inh}$	Inhaled volume rate of HW (l/min)
T_i	Average ambient temperature in a determined point (°C)
T_{globe}	Globe temperature (°C)
U	Exhaust grilles placed in the upper part of the West wall
Z	Height along the Z axis of the chamber (m)
V_i	Average absolute air velocity in a determined point (m/s)
ΔT_{prN-S}	Radiant temperature asymmetry due to the South radiant wall (°C)
ΔT_{h-f}	Temperature difference between head level (1.1 m or 1.7 m height) and feet level (0.1 m height) (°C)
ε^a	Air change efficiency index
ε_p^a	Local air change index for a determined point
ε^c	Contaminant removal effectiveness index
$\langle \tau \rangle$	Mean age of air in the room (min)
τ_n	Nominal time constant (min)
τ_p	Local mean age of air in a determined point (min)

11 **Abstract**

12 This study evaluates the convenience of the use of four different mixing ventilation configurations in
13 individual hospital rooms (IHR) based on ventilation performance and health workers (HW)
14 exposure to the contaminants released by a confined patient (CP). Two supply configurations: grilles
15 in the upper part of a wall (G) and swirl ceiling diffusers (S), combined with two different exhaust
16 grilles positions in the opposite wall: upper part (U) and lower part (D) are tested using typical IHR
17 set up. Occupants are represented by thermal breathing manikins, CP lies on a bed while HW stands
18 close to it. Three air renewal rates are tested to determine their influence in the studied variables, 6, 9
19 and 12 ACH covering the whole range of ventilation requirements of such spaces. The experimental
20 conditions considering the thermal comfort of the occupants are taken into account. Different

21 ventilation configurations create different air distribution patterns inside the room. G configurations
22 lead to high HW transient exposure values while S maintain low values that decrease when ACH is
23 increased, so this second configuration is preferred for IHRs. Results are also compared with a
24 displacement ventilation (DV) study highlighting the convenience of this strategy for IHRs.

25 **Keywords**

26 mixing ventilation; hospital room; personal exposure; ventilation effectiveness thermal comfort;
27 airborne transmission of diseases.

28 **1 Introduction**

29 Hospitals environments are risky places for cross infections because of the close interaction of
30 healthy and infected people [1]. Health workers successively visit different patients and, if they are
31 infected, can become disease vector [2]. Visitors are also in contact with patients and they can spread
32 the disease out of the hospital environment. Pathogens that spread diseases such as influenza and
33 tuberculosis can be transported through the air [3–5] being respiratory events such breathing [6],
34 sneezing [7] and coughing [8] the main exit route for it. Together with other bioeffluents, emitted
35 droplets of different size transport pathogens through the air [9]. These particles suffer an
36 evaporative effect that reduce their size until they are transformed into droplet nuclei [10–13].
37 Depending on the size of the resulting particle, it can precipitate quickly because of the effect of the
38 gravity (if its diameter is greater or 10 μm) or move through the air by means of the ventilation-
39 induced effects (in the case that its diameter is lower than 10 μm) [10]. These small particles can be
40 spread over long distances and be the cause of cross infections between people [13]. The dispersion
41 of these particles is influenced by ventilation flows [14]. Thus, a convenient ventilation strategy can
42 reduce the possibility of these infections [12,15] since it has an influence on particle dynamics [16].

43 Different types of spaces with different ventilation requirements can be present in hospitals [17].
44 Focusing our attention in individual hospital rooms (IHRs), airborne infectious isolation rooms
45 (AIIRs) as a specific configuration of IHRs, present specific ventilation requirements. While
46 recovery rooms minimal ventilation rate is fixed in 6 ACH, the requirements for AIIRs increase this
47 value to 12 ACH [17]. Patients considered highly contagious, or especially sensible to infections, are
48 confined in AIIRs. These spaces maintain a negative pressure differential with respect of the rest of
49 the building, in addition to other security measures [18] in order to maintain the patients isolated
50 from the rest of the building. Different National Health committees have published guides about
51 AIIRs design [5,19–22]. Regarding the prevention of airborne cross infections, these regulations
52 focus their attention in assuring a high ventilation air renewal rate. These recommendations are based
53 on the belief that high renewal rates could reduce cross infection risk in such spaces by diluting and
54 removing pathogens. Nevertheless, recent research focuses attention on providing a good air
55 distribution rather than on maintaining high renewal rates as being the most important factor in
56 reducing cross infection risk [15,23,24]. Thus, if this requirement is met, strategies to reduce energy
57 usage in ventilation systems by lowering airflow rates can be achieved [25]. These strategies should
58 not compromise the thermal comfort of the occupants [26,27].

59 Recent studies have tested innovative ventilation strategies such displacement ventilation (DV)
60 [28,29] and personalized ventilation [30–32] in health environments. Furthermore, more efficient
61 ventilation methods based on source control that reduce substantially the risk of exposure have been
62 suggested [17]. Nevertheless, nowadays, mixing ventilation (MV) is the most used indoor ventilation
63 strategy in such spaces, especially in IHR [19,33].

64 The configuration of the ventilation of an indoor space system has a direct influence on ventilation
65 effectiveness [34]. The ventilation efficiency in an AIIR like room has been registered for mixing
66 ventilation and 12 and 24 ACH through the local air quality index [35]. This value has been also
67 obtained numerically for different ventilation rates switching between linear and radial supply

68 diffusers for a hospital room set-up. Another numerical study analyzed ventilation efficiency values
69 for a number of combinations of wall and ceiling supply and exhaust cases in hospital rooms [36].
70 These studies highlight the influence of the relative position of the supply diffusers and exhausts on
71 the flow dynamics and hence on the ventilation performance inside the room. An experimental
72 research has been also carried out using a hospital room setup but using DV for a range of ventilation
73 rates from 6 to 12 ACH [37], showing the potential of this ventilation strategy for these spaces if it is
74 well designed, highlighting the high importance of the heat loads in air distribution for this case.
75 Different studies have obtained different occupants exposure to the exhaled contaminants of patients
76 in hospital rooms. The role of the ventilation rate in the exposure index of a health worker has been
77 studied numerically for a ceiling supply mixing configuration [23]. An experimental research have
78 been performed to evaluate the exposure the other patient in two bed hospital rooms using tracer
79 gases for MV and DV [28]. The problem has been also studied numerically for downward ventilation
80 [38] and for ceiling mixing ventilation [39]. The exposure in the positions where a health worker
81 could locate inside an isolation room have been also obtained for high ventilation rates [35], finding
82 a dependence with the negative pressure differential level in AIIRs. All these studies agree in the
83 influence of ventilation strategy and ventilation flow dynamics on patient exhaled contaminants
84 distribution. That distribution has a determinant effect on the exposure of the rest of the occupants of
85 the room. However, none of these researches studies the influence of different ventilation strategies
86 and air ventilation rates on the exposure of exhaled contaminants in a hospital room.

87 This paper presents an experimental analysis of the use of different mixing ventilation configurations
88 in a representative case of study of an IHR setup. Two different supply air configurations, through
89 grilles (G) situated at a lateral wall or through two swirl diffusers (S) placed at the ceiling. Two ways
90 to remove the exhaust air of the room have been also tested, by using two grilles placed in the upper
91 part of a lateral wall (U) or by using two grilles placed in the lower part of the same wall (D). The
92 combination of these tests make four different mixing ventilation system configurations. Three

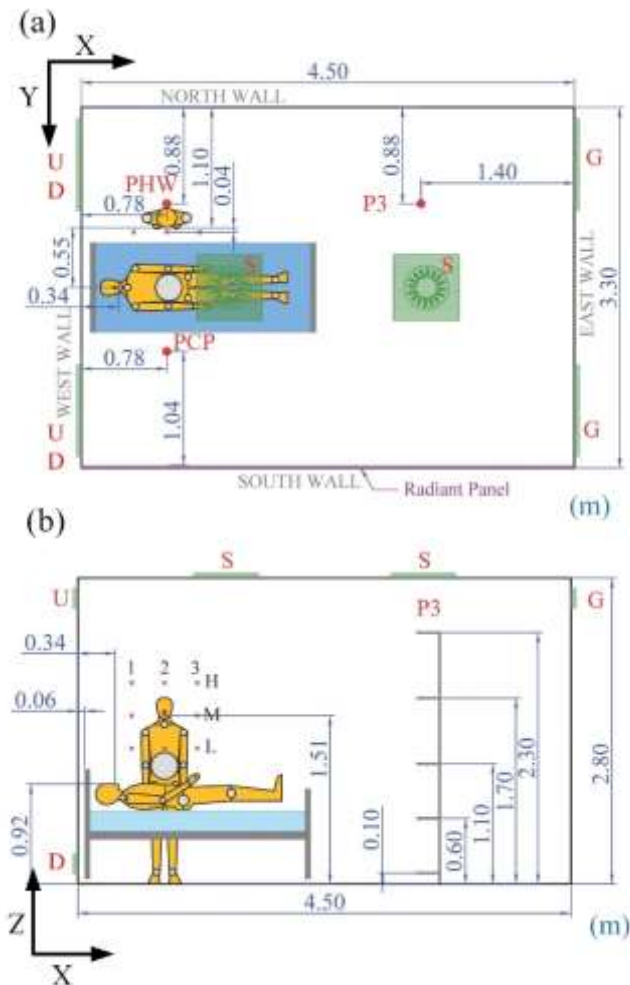
93 different air ventilation rates have been used for each ventilation configuration. The air changes per
94 hour (ACH) is switched from 6 ACH, recommended for recuperation rooms to 9 ACH and to 12
95 ACH indicated for AIIRs. The experimental setup reproduce a realistic IHR where two thermal
96 manikins representing a lying confined patient (CP) and a health worker standing close to it (HW).

97 **2 Methods**

98 Two different indicators are gathered to determine the convenience of each ventilation configuration.
99 (1) Ventilation efficiency indices and (2) HW exposure to CP exhaled contaminants and aerosols.
100 Specific experiments are carried out to determine these indicators for each ventilation configuration
101 and air ventilation rate. Ventilation efficiency indices are obtained to determine the ventilation
102 performance of each case for the IHR set-up implemented following standard methods [40].
103 Specifically air change efficiency (ϵ^a) and the local air change index (ϵ_P^a) together with the
104 contaminant removal effectiveness (ϵ^c) are obtained. HW exposure to the contaminants exhaled by
105 CP is determined by seeding CP exhalation flow with R134A as tracer gas to surrogate them. Tracer
106 gas exposition is registered in several points inside the experimental chamber and around HW
107 inhalation area. This way, the average and peak HW exposure is evaluated though different exposure
108 to contaminants (e_P^c) and intake fraction (IF) indices. To assess the transient nature of HW
109 contaminants exposure, the average of the concentration peaks and the maximum peak concentration
110 registered are also considered to obtain derived exposure indices, ($e_{P,max}^c$ and $e_{P,125\%}^c$) and (IF_{ma} and
111 $IF_{125\%}$) respectively.

112 **2.1 Test room and experimental set-up**

113 This study is carried out in an experimental chamber with a typical IHR configuration setup [37]
114 within the HVAC (heating, ventilation and air-conditioning systems) laboratory at the University of
115 Cordoba. The experimental setup can be seen at Figure 1.



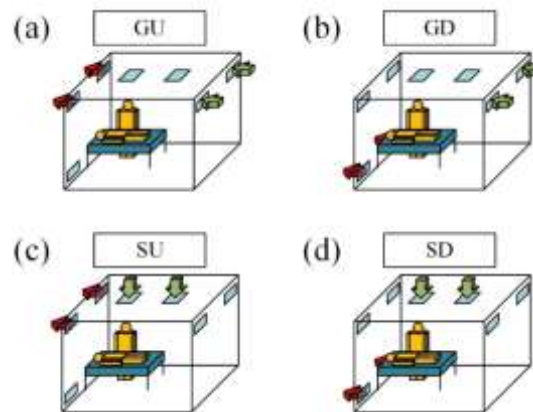
116

117 Figure 1. (a) Plan view of the test room; (b) Profile view of the test room. Ceiling swirl air diffuser (S). Wall grille air diffuser (G).
 118 Upper exhaust grilles (U). Lower exhaust grilles (D). Vertical Poles (PCP, PHW and P3). Columns of the point matrix of tracer gas
 119 measurements (1, 2 and 3). Rows of the point matrix of tracer gas measurements (H, M, L).

120 The nine points that register tracer gas concentration around the inhalation point of HW are
 121 distributed in three columns (1, 2 and 3) and three rows (H, M and L) in the same vertical plane.
 122 Rows and columns are spaced at 300 mm between each other, being the point M2 placed just in front
 123 of the mouth, center of HW, with a 4 cm gap between them, being it the inhalation point.
 124 Contaminant exposure in these points help to infer the distribution of contaminants around the
 125 breathing zone of HW and hence the routes followed by the contaminants from the exhalation of CP
 126 to HW inhalation.

127 **2.2 Ventilation configurations**

128 Clean air is supplied through two swirl diffusers, S, (VDW 400X16, Trox, Germany) or through two
129 wall grilles, G (AEH 1008X158, Trox, Germany), depending on the test carried out. Likewise, the
130 exhaust is realized through two grilles placed in the upper part of the West wall, U, or through two
131 grilles placed in the lower part of the same wall, D. U and D grilles are the same model than G ones.
132 Figure 2 shows the diagrams of the four ventilation system configurations tested in this study.



133

134 Figure 2. Ventilation system configurations tested in this study: (a) Wall grille supply combined with upper wall exhausts (GU); (b)
135 Wall grille supply combined with lower wall exhausts (GD); (c) Ceiling swirl supply combined with upper wall exhausts (SU); (d)
136 Ceiling swirl supply combined with lower wall exhausts.

137 The ventilation system has been set at three different air change rates, ACH , 6, 9 and 12 h^{-1}
138 supplying air at a supply temperature, T_s , of $18.2 \text{ }^\circ\text{C}$, $20.6 \text{ }^\circ\text{C}$ and $21.8 \text{ }^\circ\text{C}$ respectively in order to
139 maintain a mean temperature in the exhaust, T_e , of $25 \pm 1 \text{ }^\circ\text{C}$. This is done to reproduce comparable
140 and realistic IHR conditions for the tests [41]. A summary of the conditions of the three tests
141 performed can be seen at Table 1.

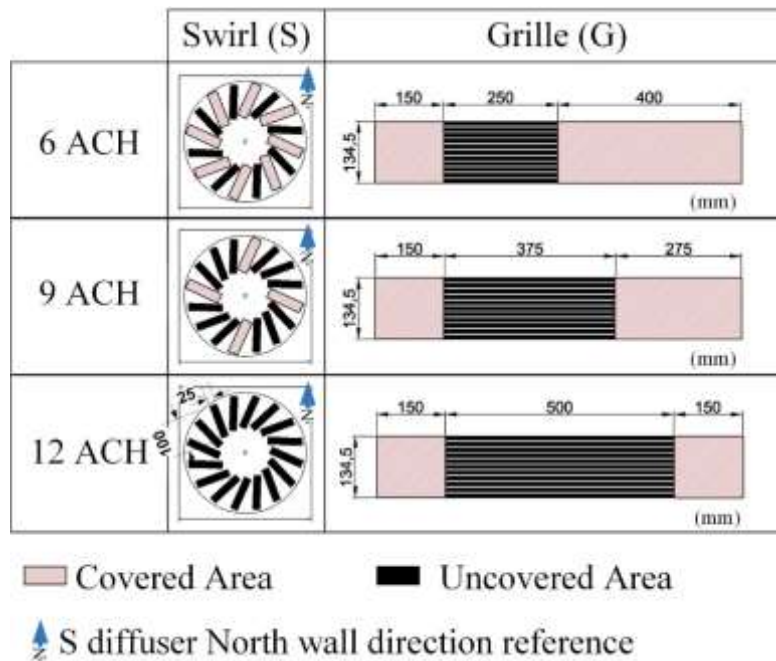
142

Table 1. Experimental conditions of the tests performed.

Renewal Rate (ACH)	Supply air flow rate (m^3/h)	Supply air temperature ($^\circ\text{C}$)
6	250	18.2
9	375	20.6
12	500	21.8

143

144 Part of the effective area of the supply diffusers is covered when 6 and 9 ACH ventilation tests are
 145 performed, Figure 3. This is necessary in order to maintain the same supply velocity and thus the
 146 same air throw in the room for all the experimental tests.



147

148

Figure 3. Supply diffuser covered area for each test performed.

149 2.3 Thermal loads and breathing thermal manikins

150 Inside the experimental chamber there are two thermal manikins representing a patient, CP, and a
 151 health worker, HW. Both manikins have the same geometry, and have been used previously in other
 152 research studies [6,37,42]. The body of the manikins is heated to achieve a homogeneous surface
 153 temperature of 34 °C which lead to the thermal gains summarized in Table 2.

154 The South wall is covered by an hydronic wall radiant system to simulate an external wall heat gain
 155 of 500 W [37]. The rest of the walls of the chamber are considered adiabatic because the temperature
 156 out of the chamber is maintained at the inward set point temperature. A summary of the thermal
 157 gains inside the experimental chamber, thermal manikins and radiant wall, can be seen at Table 2.

158

159

Table 2. Thermal gains in the experimental chamber.

Source		Load (W)	
Radiant Panel		500	
HW Manikin	Head	5.6	85
	Arms	14.4	
	Torso	19.2	
	Legs	40.8	
	Breathing	5	
CP Manikin	Head	4.9	75
	Arms	12.6	
	Torso	16.8	
	Legs	35.7	
	Breathing	5	
Total		660 W	

160

161 Each thermal manikin has its own independent breathing system with the capability of performing
 162 different breathing flows. The breathing functions characteristics of both thermal manikins are
 163 shown in Table 3.

164

Table 3. Breathing function of both thermal manikins.

Respiration frequency (min^{-1})		Minute volume (l/min)	Tidal volume (l)
In	Out		
17.90	16.43	9.46	0.55

165

166 CP exhales fresh air taken from the exterior of the experimental chamber conveniently seeded with
 167 tracer gas. In the same way HW inhales through the nose and, after analyze the tracer gas
 168 concentration of the inhaled air, it is expelled far from the experimental chamber. This way, CP
 169 manikin exhalation is the only source of contaminants present inside the experimental chamber
 170 during contaminant exposure experiments. In the same way HW can be considered the target where
 171 the contaminant exposure is evaluated.

172 **2.4 Measuring instruments**

173 Temperature, humidity and air velocity measurements are registered at different heights along three
174 different poles (PHW, PCP and P3). Table 4 summarizes the height of the different measurement
175 points, while its position on the chamber plane can be seen in Figure 1.

176 Table 4. Probes position along the height of each pole.

Height (m)	P3 Pole	PHW Pole	PCP Pole
2.3	T_i	T_{ib}, V_i	T_{ib}, V_i
1.7	T_i	T_{ib}, V_{ib}, HR_i	T_{ib}, V_{ib}, HR_i
1.1	T_i	T_{ib}, V_i	T_{ib}, V_i
0.6	T_i	T_{ib}, V_i	T_{ib}, V_i
0.1	T_i	T_{ib}, V_i	T_{ib}, V_i

177

178 Ambient temperature probes (T_i) consist of J-type thermocouples with an accuracy of 2% in the
179 range 15 – 45 °C. Absolute air velocity (V_i) is measured using hot-sphere anemometers (TSI Air
180 Velocity Transducer 8475, TSI, Minnesota) with a 3% accuracy in the range of 0.02 to 2.5 m/s.
181 Ambient relative humidity (HR_i) has been measured using air humidity sensors (HMT100, Vaisala,
182 Finland) with a calibration accuracy of 1.7% on the full range 0-100%.

183 The temperature of the inner surfaces of the chamber is registered during the tests by means of 15
184 resistive temperature probes (PT100, TC Direct, UK). Using the inner enclosure average
185 temperatures, radiant temperature is calculated using the method B.4.2 of EN ISO 7726 standard
186 [43]. These probes have been calibrated in the range from 20 to 40°C to assure an accuracy of
187 $\pm 0.3^\circ\text{C}$.

188 Tracer gas equipment is used to study the exposure of manikin HW to the contaminants exhaled by
189 CP manikin. R134a is selected as a tracer gas as it has been done in similar previous studies
190 [37,44,45]. To dose the tracer gas emitted through CP exhalation and register tracer gas
191 concentration around HW manikin close environment, a multipoint sampler and doser (Innova 1303,

192 LumaSense Technologies, California) along with a photoacoustic gas monitor (Innova 1412,
193 LumaSense Technologies, California) are used.

194 Smoke has been introduced in the room completely mixed with the supply ventilation air through the
195 diffusers in order to analyze airflow distribution inside the chamber in each case. A commercial
196 specific fluid (Normal Power Mix, Safex, Germany) is used on the smoke generator machine
197 (F2010Plus, Safex, Germany). Videos have been recorded using a digital video camera (DSC-H50,
198 SONY, Japan). All the edited videos have been added as Supplementary Information.

199 **2.5 Thermal comfort indices**

200 The procedures detailed in ISO EN 7730 [46] are used to determine different thermal comfort indices
201 for the position of PCP and PHW poles. A standing person performing a light activity, standing (1.4
202 met), is considered in PHW pole position while for the PCP pole a sitting one is considered, seated
203 quiet (1 met). According to the usual light clothing conditions in hospitals, a clothing level index of
204 0.57 clo, trousers and short sleeved T-shirt, is assumed [47].

205 In order to determine general thermal comfort operative temperature (T_o) and the predicted mean
206 vote (PMV) - predicted percentage of dissatisfied (PPD) values are obtained. Local thermal
207 discomfort is also considered by means of the gathering of different indices. The radiant temperature
208 asymmetry between the South and North the walls ($\Delta T_{pr,N-S}$), where a radiant panel simulates an
209 external thermal gain . The draft discomfort is evaluated through the draught local discomfort (DR).
210 Finally, the temperature difference between the head and feet (ΔT_{hf}) is gathered to assess the
211 discomfort due to the temperature gradient along the height of the chamber.

212 **2.6 Ventilation performance indices**

213 In order to determine the effectiveness of the ventilation, two ventilation efficiency indices have
214 been used, air change efficiency (ε^a) and the local air change index (ε_p^a). The first index evaluates

215 the ventilation efficiency globally while and the second determines its performance in a determined
216 point. The expressions used to define these indices are:

$$\varepsilon^a = \frac{\tau_n}{2 \cdot \langle \tau \rangle} \cdot 100 \quad (1)$$

$$\varepsilon_p^a = \frac{\tau_n}{\tau_p} \cdot 100 \quad (2)$$

217
218 Being, τ_n the nominal time constant, τ_p the local mean age of air and $\langle \tau \rangle$ is the chamber mean age of
219 air. The step down method [40] is used to determine the times involved in the indices, being 40 ppm
220 the initial concentration chosen. Tracer gas concentration is registered over time in the exhaust to
221 obtain ε^a and in three different points around HW inhalation surroundings (M1, M2, and M3) to
222 obtain ε_p^a .

223 The contaminant removal effectiveness index (ε^c) is obtained for the whole chamber with the
224 purpose of determining global contaminant removal performance of the contaminants emitted
225 through CP exhalation. Contaminants are surrogated by R134A as a tracer gas which is seeded
226 completely mixed with CP exhalation flow at a concentration of 7382 ppm. Contaminant removal
227 effectiveness index has been previously obtained in recent studies [36,44,45,48]. Its value is obtained
228 as follows:

$$\varepsilon^c = \frac{\bar{c}_e - \bar{c}_s}{\langle \bar{c} \rangle - \bar{c}_s} \quad (3)$$

229 Where $\langle \bar{c} \rangle$ represents the mean concentration of contaminant of the chamber and \bar{c}_e and \bar{c}_s represents
230 the mean contaminant concentrations in the exhaust and in the supply respectively. The value of $\langle \bar{c} \rangle$
231 is obtained immediately after the stationary experiment finishes by shutting down the ventilation
232 system and mixing the air inside the chamber using an auxiliary fan [40].

233 **2.7 HW tracer gas exposure**

234 In order to determine the exposure of HW to the contaminants emitted by CP, its exhalation is seeded
235 with tracer gas as it was previously detailed in ε^c evaluation method. Tracer gas concentration is

236 registered in 9 points around HW inhalation surroundings distributed in three columns (1, 2 and 3)
 237 and 3 rows (H, M and L) as can be seen in Figure 1. Additionally, the concentration is also recorded
 238 inside the inhalation of HW airway. Each test is performed stationary during 6 hours after steady
 239 state conditions are obtained inside the chamber. In order to be sure that the experimental exposure
 240 time is enough to obtain representative values of the tracer gas exposure, a detailed analysis have
 241 been carried out. The results are shown in a Supplementary Information section.

242 The concentration measurement along the time in each point (P) is used to calculate the
 243 concentration mean value, (\bar{c}_P), and the concentration maximum value, ($c_{P,max}$). Since it has been
 244 observed that concentration peaks arise in different points in a transitory way, the average peaks
 245 concentration ($\bar{c}_{P,125\%}$) and its frequency ($f_{P,125\%}$) are defined to describe this circumstance. A peak
 246 is considered when its value exceed the 125% of the average value of the concentration.

247 Two derived exposure indices, exposure to contaminants (e_P^c) and intake fraction (IF) are obtained
 248 to evaluate the exposition of HW to the contaminants released by CP.

249 The exposure to contaminants (e_P^c) relates the local contaminant concentration with the difference
 250 between average one obtained in the exhaust (\bar{c}_e^c) and in the supply (\bar{c}_s^c). Contaminant concentration
 251 in the supply is always is always null because the tracer gas used can't been found naturally in the
 252 atmosphere. This index is obtained for each contaminant index \bar{c}_P , $\bar{c}_{P,125\%}$ and $c_{P,max}$, to obtain e_P^c ,
 253 $e_{P,125\%}^c$ and $e_{P,max}^c$ as follows:

$$e_P^c = \frac{\bar{c}_P - \bar{c}_s}{\bar{c}_e - \bar{c}_s}; e_{P,125\%}^c = \frac{\bar{c}_{P,125\%} - \bar{c}_s}{\bar{c}_e - \bar{c}_s}; e_{P,max}^c = \frac{c_{P,max} - \bar{c}_s}{\bar{c}_e - \bar{c}_s} \quad (4)$$

254

255 Additionally, intake fraction (IF), which is the ratio of the mass of a pollutant inhaled to the mass of
 256 the pollutant emitted seeded in CP exhalation at a certain concentration ($\bar{c}_{CP,exh}$), is evaluated for
 257 the measuring point placed inside the inhalation airway of HW (Inh). This index is obtained for each

258 contaminant value \bar{c}_P , $c_{125\%}$ and $\bar{c}_{P,maxk}$, to obtain IF , $IF_{125\%}$ and $IF_{max}:(Inh)$. The equations used
259 are the following:

$$IF = \frac{\int Q_{b,inh} \cdot c_{inh} dt}{\int Q_{b,exh} \cdot c_{CP,exh} dt}; IF_{125\%} = \frac{\int Q_{b,inh} \cdot c_{inh,125\%} dt}{\int Q_{b,exh} \cdot c_{CP,exh} dt}; IF_{max} = \frac{\int Q_{b,inh} \cdot c_{inh,max} dt}{\int Q_{b,exh} \cdot c_{CP,exh} dt} \quad (5)$$

260

261 Where $Q_{b,inh}$ and $Q_{b,exh}$ are the inhaled and exhaled breathing flows of the manikins respectively.

262 Since both manikins perform the same breathing function, the intake fraction expression can be

263 simplified to the quotient between the average tracer gas concentration value in the inhalation airway

264 of HW (\bar{c}_{inh}) and the tracer gas concentration emitted through CP exhalation ($\bar{c}_{CP,exh}$). The value of

265 $\bar{c}_{CP,exh}$ is obtained averaging the tracer gas concentration measurements registered inside the

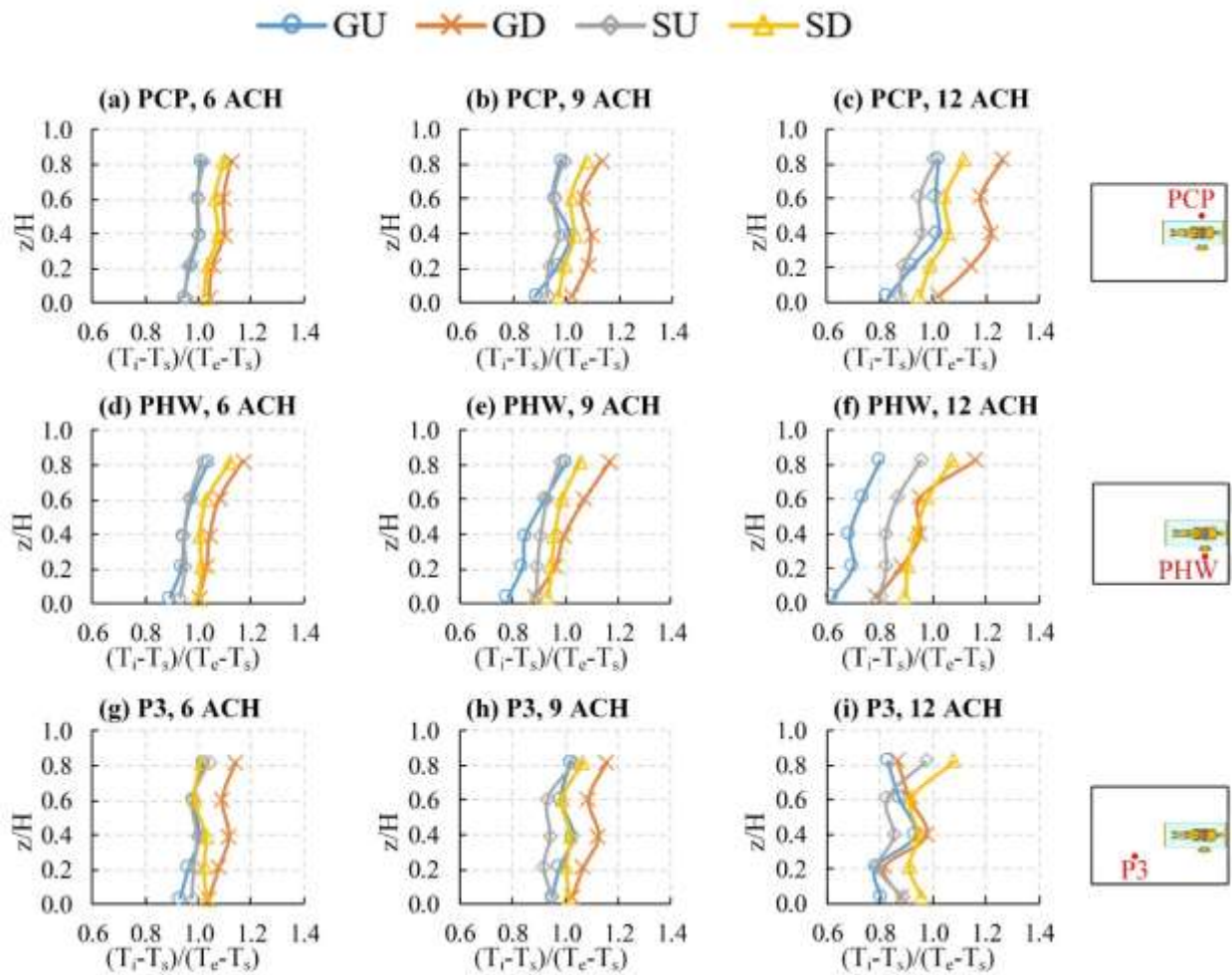
266 exhalation airways of CP during a 6 h experiment. The values of $IF_{125\%}$ and IF_{max} are calculated

267 replacing \bar{c}_{inh} by $\bar{c}_{inh,125\%}$ and $\bar{c}_{inh,max}$ respectively.

268 **3 Results and discussion**

269 **3.1 Experimental conditions**

270 The vertical temperature gradients measured for the four experiments at the three poles of the
 271 room: PCP, PHW and P3 are shown in Figure 4.



272

273 Figure 4. Non dimensional profiles of temperature along the three vertical poles of the room, PCP, PHW and P3 for different
 274 ventilation system configurations, GU, GD, SU and SD, and different air change rates, 6 9, and 12 ACH.

275 Results show a similar temperature distribution along the three temperature poles for each
 276 experiment. Dimensionless temperature profiles show, in general, a slight positive gradient with
 277 height in all cases, that is higher when the extraction of the air is made by the lower exhaust grilles
 278 (D). This may be due to a difficult of the warm air to find the exhaust in an area affected by the
 279 thermal convection of the manikins. According to the results, the use of the upper exhaust grilles (U)

280 lead to lower relative temperature values. The differences between the obtained profiles are more
 281 evident when the ventilation rate is increased especially for PCP and PHW profiles. These
 282 differences could be a consequence of different airflow distributions patterns generated by each
 283 ventilation system.

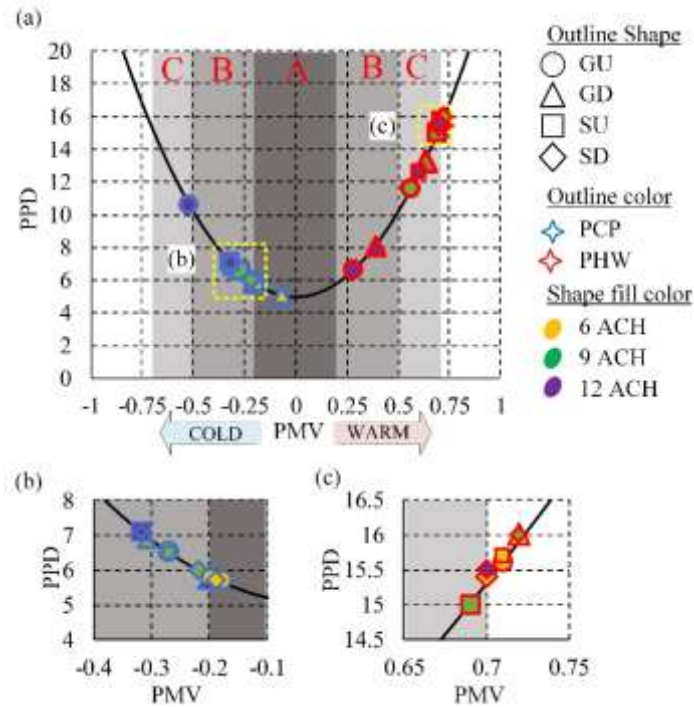
284 Global and local comfort indices are evaluated for two positions inside the chamber, PHW and PCP,
 285 see Figure 1. Results have been summarized in Table 5.

286 Table 5. General and local thermal comfort indices for health worker (PHW) and patient (PCP) under different ventilation
 287 configuration and different air changes per hour, ACH.

		PHW						PCP					
		T_o	PMV	PPD	ΔT_{prN-S}	ΔT_{h-f}	DR	T_o	PMV	PPD	ΔT_{prN-S}	ΔT_{h-f}	DR
		°C	-	%	K	K	%	°C	-	%	K	K	%
GU	6	25.7	0.71	15.6	0.8	0.5	2.6	26.0	-0.18	5.7	2.3	0.4	1.1
	9	25.4	0.56	11.6	0.6	0.6	7.3	25.8	-0.27	6.5	2.2	0.6	3.4
	12	24.6	0.28	6.6	0.7	0.3	13.9	25.5	-0.52	10.6	2.4	0.6	7.5
GD	6	26.1	0.72	16	0.7	0.5	7.0	26.3	-0.07	5.1	2.1	0.4	2.0
	9	25.6	0.63	13.3	0.5	0.7	6.1	25.8	-0.31	6.9	2.2	0.3	5.5
	12	25.2	0.39	8.1	0.7	0.4	15.5	25.9	-0.2	5.8	2.1	0.5	5.5
SU	6	25.7	0.71	15.7	0.3	0.3	0.0	26.0	-0.2	5.8	1.9	0.3	3.5
	9	25.6	0.69	15	0.4	0.2	4.6	25.9	-0.27	6.5	1.9	0.2	5.6
	12	25.4	0.6	12.6	0.4	0.3	6.1	25.8	-0.32	7.1	2.0	0.3	5.8
SD	6	25.7	0.7	15.4	0.4	0.3	0.0	26.0	-0.19	5.7	2.0	0.3	0.0
	9	25.8	0.72	16	0.3	0.3	2.2	26.0	-0.22	6	1.9	0.3	6.4
	12	25.7	0.7	15.5	0.4	0.3	2.3	26.0	-0.32	7.1	1.9	0.3	7.5

288
 289 Results show that T_o decreases slightly when air ventilation rate increases. That means that the
 290 increase of the air ventilation rate has an impact on the T_o at the poles positions. This effect is more
 291 evident when G supply is used, being both PCP and PHW pole positions exposed to this effect. This
 292 is due to the increase of the air velocity in the occupied zone when the air ventilation rate is
 293 increased as the increment of the DR index for G tests indicates. It does not happen in S tests
 294 presumably because of the different flow distribution originated by this diffuser. Anyway, the values
 295 obtained are situated in the comfort zone for summer clothing and sedentary activity for low relative
 296 humidity situations [46,49].

297 General thermal comfort indices summarized in Table 5 have been plotted in Figure 5 for better
 298 understanding, where thermal comfort categories are defined according to the standard EN ISO 7730
 299 [46].



300

301 Figure 5. Predicted percentage of dissatisfied (PPD) as a function of predicted mean vote (PMV) for different ventilation
 302 configurations and different air changes per hour; (a) Full range of results; (b) Detail view of some of PCP results; (c) Detail view of
 303 some PHW results.

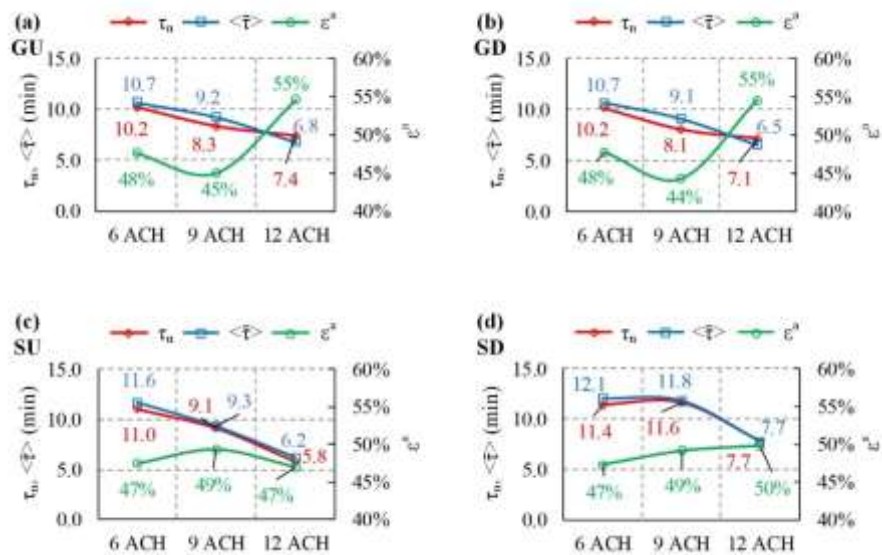
304 According to the results, thermal comfort indices PMV for PCP and PHW positions differs in all the
 305 cases. PMV indices for PCP position reflects a slightly cold sensation, in most cases between the
 306 categories A and B. Nevertheless, for PHW position, this index reflects a warm sensation, which
 307 even overpass C category in some cases as it can be seen at Figure 5 (c). This is directly related with
 308 the different activity levels considered in each pole. Results suggest that the increase in ventilation
 309 rate lead to colder sensations in all cases.

310 To assess completely comfort in the room, different local discomfort indices have been obtained and
 311 presented in Table 5. Radiant temperature asymmetry due to South radiant wall, ΔT_{prN-S} , is higher in
 312 PCP position due to its proximity to the South wall. The increase of the ventilation rate does not lead
 313 to different values of ΔT_{prN-S} . It can be also noted that the use of the S supply reduces ΔT_{prN-S} and

314 ΔT_{h-f} indices. It can be due to the effect of the S diffuser on the radiant wall. The value of DR
 315 increases with the air ventilation rate. It is because the increase of the average air velocity generated
 316 by the increase of the air ventilation rate. The effect is more evident for G supply ventilation
 317 configurations and PHW position. The different ventilation airflow rate could modify the air
 318 distribution patterns inside the room making the air reach directly the standing person head height at
 319 PHW position, increasing local discomfort in this case.

320 3.2 Ventilation performance

321 The values of τ_n , $\langle \bar{\tau} \rangle$ and ε^a have been obtained for each ventilation configuration. Results are
 322 shown in Figure 6.



323

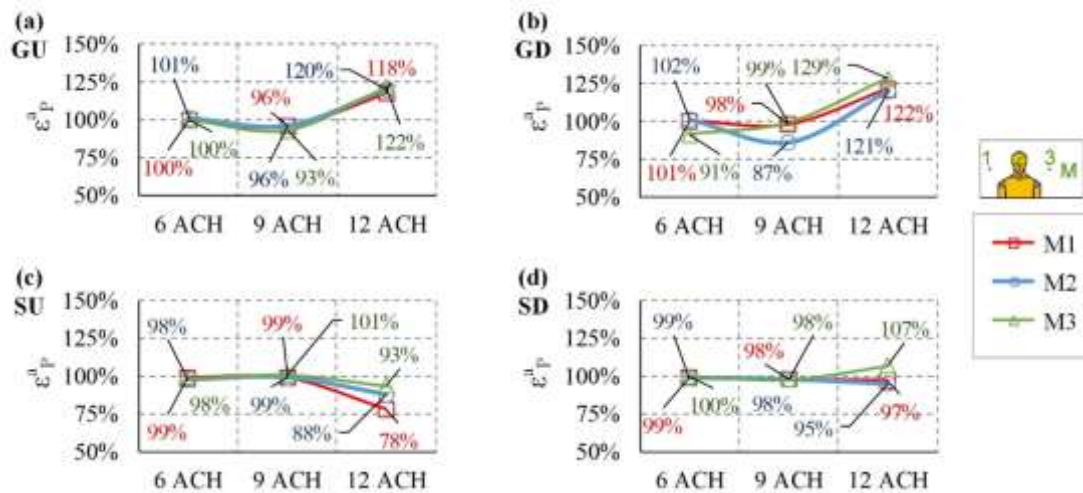
324 Figure 6. Air change efficiency (ε^a), nominal time constant (τ_n) and room mean age of air ($\langle \bar{\tau} \rangle$) for the four ventilation configurations
 325 considered at different air change rates. (a) GU; (b) GD; (c) SU; (d) SD.

326 According to the results obtained, the value of ε^a is around 50% in all cases. If this value is reached,
 327 a perfect mixing situation is found [40]. The values of τ_n and $\langle \bar{\tau} \rangle$ times tend to decrease when the
 328 ventilation rate increases. This decreasing tendency is different for each ventilation configuration.
 329 The value of $\langle \bar{\tau} \rangle$ is higher than τ_n in all cases except for G supply when 12 ACH is tested, being this
 330 the only case where ε^a exceeds 50%. That means that the contaminants are evacuated quickly
 331 through the exhaust remaining short time inside the room. However, it is found that ε^a barely reach

332 45% when G supply is used in 9 ACH tests. That means that the contaminants take more time to
 333 leave the room, this way contaminants have the possibility of being stacked inside.

334 When S supply is chosen, the value of ε^a remains close but under 50% for all the air changes used. It
 335 can be noted that the increase of air ventilation rate improve ε^a value in SD cases but not in SU ones.
 336 Even so, in both configurations, the differences of ε^a for the different ACH tested are lower than in
 337 G supply cases.

338 The results of ε_p^a values are obtained in three points in the near surrounding of HW inhalation area,
 339 M1, M2 and M3 and are shown in Figure 7.



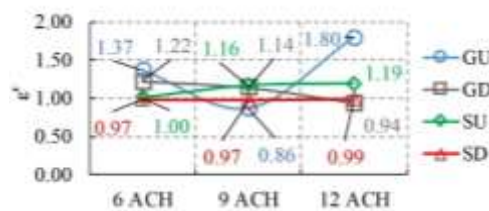
340
 341 Figure 7. Local air change index (ε_p^a) for three points around HW inhalation point at different air change rates. (a) GU ventilation
 342 strategy; (b) GD ventilation strategy; (c) SU ventilation strategy; (d) SD ventilation strategy.

343 The values of ε_p^a remains close to 100% for all the tests performed. It means that the air is well
 344 mixed in the local area around HW inhalation area as in the whole room. Differences in ε_p^a between
 345 the configurations tested are found especially at higher ventilation rates. When G supply is used the
 346 value of ε_p^a tends to decrease for 9 ACH, especially for GD test in M2, to afterward increase to about
 347 120% for 12 ACH one. That means that contaminants remain more time in the surroundings of HW
 348 when 9 ACH are performed than in the cases of 6 and 12 ACH. These fluctuations in ε_p^a values can
 349 be due to changes in air distribution patterns inside the room when the ACH value is modified.

350 In S supply cases, a higher dispersion of results is found under 12 ACH ventilation rate, in contrast
 351 with the data homogeneity of the 6 and 9 ACH tests. When the ventilation rate is high, a stronger
 352 swirl downward flow from the diffusers could be breaking the arising convective flow from CP
 353 manikin body. This way, the horizontal spreading of contaminants is promoted, leading to different
 354 contaminants concentration in the three points considered.

355 In both G and S supply configurations, no improvement is found in ε_p^a when the ventilation rate is
 356 increased from 6 to 9 ACH. When the ventilation rate is increased to 12 ACH the value of ε_p^a
 357 increases under G supply configuration while in S cases its value becomes dependent on the position.

358 In order to analyze how contaminants are globally removed by each ventilation configuration, ε^c
 359 index is obtained. To do this, the average contaminant concentration in the room ($\langle \bar{c} \rangle$) and in the
 360 exhaust (\bar{c}_e) have been registered for all the tests carried out. Results are shown in Figure 8.



361

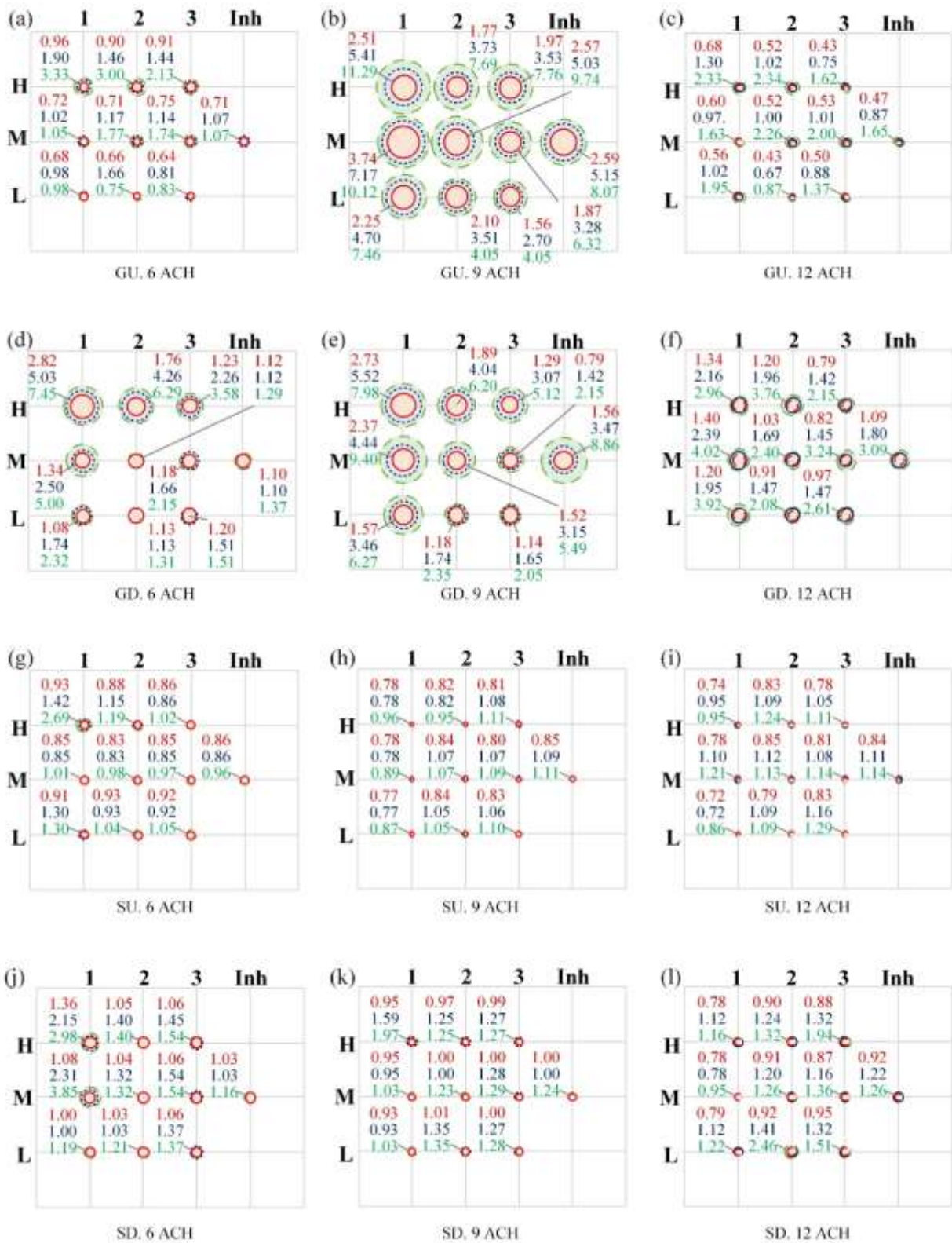
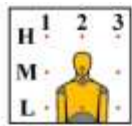
Figure 8. Contaminant removal effectiveness (ε^c) index for the four ventilation configuration tested.

362

363 According to the results, the values of ε^c remains around 1 for nearly all the tests. The values for GD
 364 and SU maintain values over the unit while SD values are slightly under the unit. This might be due
 365 to the difficult of the upward exhaled contaminants to reach the D exhaust placed in the lower part of
 366 the room. The case of GU is different to the rest, for 12 and 6 ACH it performs the highest values of
 367 ε^c . This is positive because it means that the contaminants path to the exhaust is relatively short and
 368 quick. However, for GU with 9 ACH the lowest value of ε^c is obtained. It can be due to the short
 369 circuit generated between the G supply grilles and the exhausts grilles placed at the same height in
 370 the opposite wall. In that way, the airflow from the supply grilles is not able to reach the CP
 371 exhalation area and remove efficiently the contaminants exhaled.

372 **3.3 HW tracer gas exposure**

373 Tracer gas exposure is evaluated in 9 points around the inhalation of HW and in the inhalation of
374 HW (*Inh*), as it can be seen in Figure 1. Figure 9 shows the values of e_p^c , $e_{p,125\%}^c$, and $e_{p,max}^c$ for
375 these points.



376

377
378

Figure 9. Local relative contaminant exposure coefficient (e_p^e), local relative average peaks concentration exposure coefficient ($e_p^e,125%$) and maximum peak exposition coefficient (e_p^e,max) for the tests carried out. (a) GU 6 ACH; (b) GU 9 ACH; (c) GU 12

379 ACH; (d) GD 6 ACH; (e) GD 9 ACH; (f) GD 12 ACH; (g) SU 6 ACH; (h) SU 9 ACH; (i) SU 12 ACH; (j) SD 6 ACH; (k) SD 9 ACH;
380 (l) SD 12 ACH.

381 According to the results, there is a notable difference between the results obtained for G supply tests
382 and the ones obtained for S supply. In general terms, it can be noted that the exposure indices are
383 higher in the cases where G supply is used. S supply tests maintain homogeneous e_p^c values in all the
384 points, and in most of them the value is the same that $e_{p,125\%}^c$ and very close to 1. The values of
385 $e_{p,max}^c$ show values not far from e_p^c in all cases, revealing a high homogeneity over time for
386 contaminant concentration. It can be noted that exposure indices show lower values for SU in
387 comparison with SD.

388 In contrast, G supply exposure values behaves in a very different way, showing in some cases high
389 discrepancies between exposure values depending on the position, the *ACH* and the height of the
390 exhaust. GU 9 ACH stands out as the case where the exposition is higher in all the points around the
391 HW and in its inhalation. The explanation might be found in the ventilation flow distribution inside
392 the chamber. The clean air from the grille diffusers is not able to remove the exhaled contaminants
393 from the occupied zone maybe due to a short circuit produced between the grilles and the exhausts
394 for that case. Figure 10(b) shows a capture from the smoke test video showing the ventilation flow
395 development for this case, reinforcing this theory. The flow reaches the upper part of the West wall
396 where part of it leaves directly the room, being short circuited. This situation produce a stagnation of
397 the contaminants around HW inhalation area. The results are compatible with the results obtained for
398 ε^c that suggested that part of the contaminants are stacked into the room. However, for the same GU
399 ventilation configuration under 6 and 12 ACH, low values of exposition in all the points are
400 obtained. For 6 ACH case, the clean airflow from the grilles moves downward to the exhalation area
401 improving the mixing process of the exhaled contaminants and reducing the exposure indexes, as it
402 can be seen in Figure 10(a). When using 12 ACH, the volume of clean air increases and generates a
403 strong upward flow in the occupied area situated between the inlets and the outlets of the room, as a

404 result of its reaching of the West wall, Figure 10(c). This airflow pattern conduces the exhaled
405 contaminants quickly to the exhausts generating a low risk of exposure to HW.



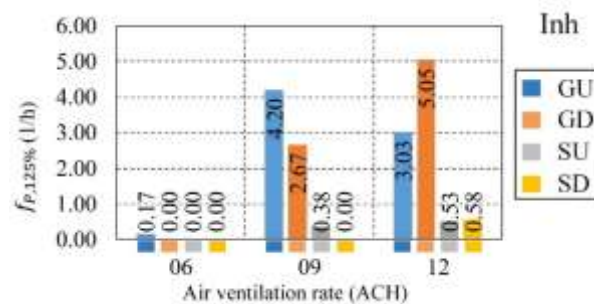
406

407 Figure 10. Video frame captures showing throw development of the GU tests. (a) GU 6 ACH; (b) GU 9 ACH; (c) GU 12 ACH.

408 Some points with high contaminants exposure values can also be found for GD ventilation
409 configuration. These points are found for 6 and 9 ACH cases. For GD 6 ACH case, high exposure
410 points distribute at H positions, situated at the height of HW head. In this case the clean airflow
411 coming from inlets could be displacing contaminants to the West wall going upward to the area of
412 the HW head. However this fact maintains the breathing area of HW clean of contaminants. For the
413 case of GD 9 ACH the clean airflow from the grilles interacts with the upward convective flow from
414 the manikins making difficult for the exhaled contaminants to find the exhaust and creating a
415 stagnant area. This fact produces a direct influence of the patient exhalation in the contaminant
416 inhalation of HW. The average values of exposure (e_p^c) and the maximum values of exposure
417 ($e_{p,max}^c$) show a significant difference. This situation changes when 12 ACH is set due to the
418 increase of air volume that penetrates into the exhalation area in despite of the ascending thermal
419 plumes leading the contaminants directly to the exhaust. Previous research on exposure to
420 contaminants released by respiratory events reinforces the idea that an increase of ACH doesn't
421 necessary leads to a better contaminants exposure indices due to the changes that it produces in
422 airflow patterns inside the indoor space [50–52].

423 In general for G supply cases, the points where a high exposure value is obtained show a high
 424 discrepancy between e_p^c , $e_{p,125\%}^c$ and $e_{p,max}^c$. That reveals that the high contaminants exposure
 425 registered is not constant in time but it reveals a transient nature. High contaminant concentration
 426 exposure peaks $e_{p,125\%}^c$ arise without any evident periodicity. This situation could be related with the
 427 fact that contaminants are not released constantly but they are seeded into CP exhalation flows. That
 428 means that the peaks are not homogeneous, being possible high values of $e_{p,max}^c$ with low values of
 429 e_p^c . In the inhalation area for GD and 9 ACH the $e_{p,max}^c$ is more than 5 times the e_p^c . These two facts
 430 reinforce the idea that despite the conditions of the problem are stationary, the exposure to the
 431 contaminants reveals a transient nature.

432 The frequency of the peaks ($f_{p,125\%}$) registered inside the airways of HW (*Inh*) is shown in Figure
 433 11.



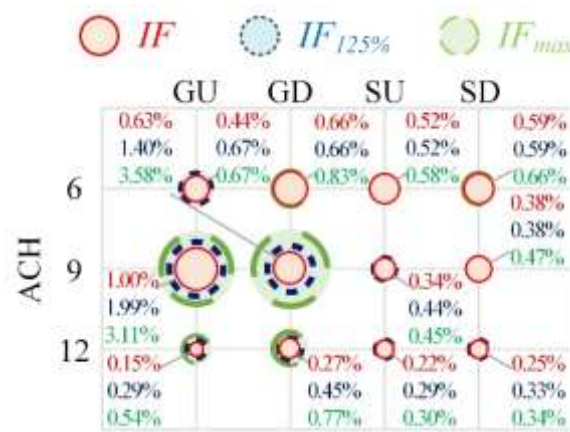
434

435 Figure 11. Frequency of maximum exposure coefficients ($e_{p,max}$) inside the airways of HW.

436 The swirl diffusers used for SU, SD cases avoid the tracer gas peak concentration in the inhalation
 437 due to an effective dilution of the contaminants emitted by CP. This way the direct influence of the
 438 exhalation on the breathing area of the HW is avoided, maintaining low $f_{p,125\%}$ values. For G
 439 supply, it exists a dependency between the air ventilation rate and the $f_{p,125\%}$ value. Very low values
 440 of $f_{p,125\%}$ are found when 6 ACH ventilation rate is performed showing a dilution process of the
 441 contaminants exhaled. On the contrary, $f_{p,125\%}$ increases for 9 and 12 ACH. This fact shows that the
 442 mixing process in the occupied area is not being complete and therefore there is an influence of P

443 exhalation on the breathing area of HW. The high values of $f_{P,125\%}$ combined with the high values of
 444 $e_{P,125\%}^c$ indicates a high risk of exposure. However, for GU and GD under 12 ACH the high values
 445 of $f_{P,125\%}$ are not related with high values of exposure since the values of $e_{P,125\%}^c$ are low. That
 446 means that also there is an influence of CP exhalation on the breathing area of HW when the
 447 occupied zone is maintained clean of contaminants.

448 The value of IF index is obtained to evaluate the amount of contaminants that are inhaled by HW
 449 respect to the amount exhaled by CP. Results are shown in Figure 12.



450
451 Figure 12. Intake Fraction.

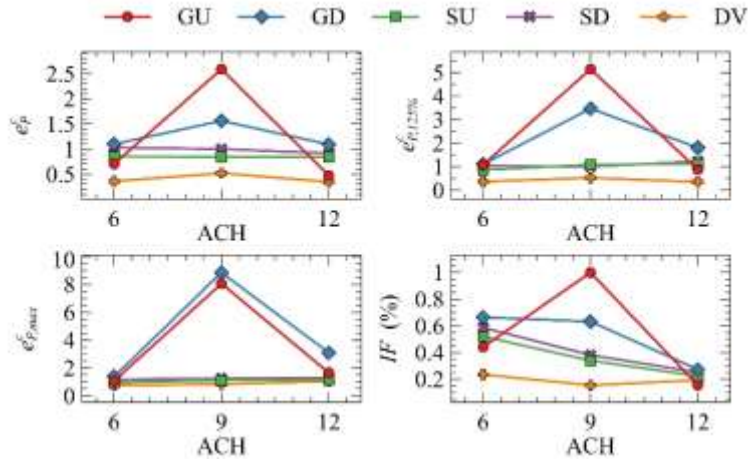
452 Results show that the ventilation configurations tested present, in general, a similar decreasing IF
 453 tendency with the increasing of the air ventilation rate. The more volume of clean air entering the
 454 room, the less percentage of inhaled contaminants relative to the exhaled contaminants. The case of
 455 GU 9 ACH presents the only exception for this tendency due to a direct influence of the
 456 contaminants released by CP in the inhalation area of HW. The airflow pattern generated during this
 457 test maintains the exhaled contaminants released by CP in the breathing area of HW, making it
 458 difficult for the contaminants to evacuate the room through the exhausts. This phenomenon
 459 disappears when air ventilation rate is increased to 12 ACH, decreasing considerably the value of IF .
 460 When GD configuration is used, the values of IF are also high for 6 and 9 ACH. It has been
 461 observed for these tests that it is difficult for the exhaled contaminants to find the way to the exhaust.

462 This fact may be due to the interaction between the upward flow of the manikin's thermal plumes
463 and the downward flow generated by this ventilation strategy. The values of IF and $IF_{125\%}$ show
464 discrepancies which reveals that the high exposure is due to punctual peak concentrations episodes.
465 The value of IF_{max} is also quite higher than $IF_{125\%}$, so it can be stated that the peaks reach different
466 values over the time. IF_{max} can even reach values five times higher than IF ones such in the case of
467 GU 9 ACH. The cases where S supply is used, IF values present a constant decreasing tendency,
468 being in most cases the values of $IF_{P,125\%}$ and IF_{max} very close to IF . This shows that the dilution of
469 the CP exhaled contaminant maintain a low and homogeneous tracer gas concentration in HW
470 inhalation. It has been also noted that the IF values are somewhat lower for SU tests.

471 **4 Discussion**

472 This work examines the effectiveness of different mixing ventilation strategies in the removal of
473 contaminants in an IHR analyzing different indexes.

474 The mixing ventilation study has been performed using the same experimental setup, thermal gains
475 disposition and experimental equipment and methods than a previous study based on displacement
476 ventilation (DV) [37]. Three different air changes per hour are performed for each ventilation
477 strategy, which consider two different inlet diffusers: wall grilles (G) and swirl diffusers (S), and two
478 different exhausts positions: in the lower part of the wall (D) and in the upper part of the wall (U).
479 That leads to a total of 12 experimental cases studied. The results obtained are of significant
480 relevance in order to understand which ventilation strategy will lead to a less risk of exposure to
481 exhaled contaminants in a IHR. The risk of exposure is obtained for a health worker (HW) placed
482 close to the patient (CP) which is considered the source of exhaled contaminants. Figure 13 shows a
483 comparison of the exposure indices for the different ventilation strategies, GD, GU, SD, SU and DV,
484 in an IHR for Inh point placed inside the inhalation airway of HW.



485

486
487

Figure 13. Comparison between exposure indices at Inh point. (a) Local relative contaminant exposure index (e_p^c); (b) Average of peaks relative exposure index ($e_{p,125\%}^c$); (c) Maximum peak exposure index (e_{max}^c); (d) Intake fraction (IF).

488

Firstly, it is possible to see that the displacement ventilation strategy (DV) shows the best index value with very low exposure of HW for all the exposure indices analyzed. This result is in agreement with previous studies of displacement ventilation [28,53] where it is possible to find low values of the risk of infection with that strategy. In this particular case, the position of the source of contaminants (exhalation of the patient) in a lower position respect to the HW breathing area improve the results. The thermal stratification of the displacement ventilation system maintains the exhaled contaminants in a layer below the breathing area of the HW. Different relative position of the manikins may lead to completely different results.

496

Secondly, if we observe the results obtained for SD and SU, for the three ACH performed, both strategies show values typical of a complete mixing process, close to 1. The mixing process is complete and independent of the number of ACH. Nevertheless, a slight dependence of the exhaust positions is observed, SU performs slightly better than SD in contaminant removal and HW exposure indices. The values of ϵ^c together with e_p^c and IF exposure values suggest that part the tracer gas concentration inside the chamber remains higher in SD cases due the exhaust position.

502

Finally, high exposure values depending on the number of ACH and the position of the exhausts has been found in GD and GU cases. Considering GD and GU 9 ACH cases, the exhaled contaminants

503

504 remain close to the breathing area of HW, increasing its exposure to contaminants. However, when
505 12 ACH in GD and GU cases, the increase of airflow decreases its exposure. This result points out
506 that a specific study of a particular case, taking into account: position of the thermal loads, position
507 of the inlets and exhausts, distance between the manikins, and relative positions between all these
508 relevant parts of the room, may play the crucial role in understanding the risk of airborne exposure of
509 people in a room.

510 **4.1 Limitations of the work**

511 It is important to bear in mind that the results obtained and discussed in this work are obtained under
512 specific experimental conditions. The relative position of the source of contaminants, the different
513 positions of the inlets and exhausts or different distances between the manikins may change the
514 conclusions obtained. In the same way, the height at which the contaminants are exhaled plays a
515 crucial role in the exposure to contaminants of the HW, especially for the DV system.

516 The experimental set up has not been carried out in a real hospital and the problem only treats tracer
517 gas as a strategy to simulate small droplet nuclei, not real biological contaminants. The experimental
518 results are not showing a complete real situation since the manikins are also steady. However, all the
519 results analyzed could be helpful in the design of IHRs in order to create environments where the
520 exposure to exhaled contaminants may be reduced in most of the situations.

521 The tracer gas measurement sample rate is lower than the periodic breathing process time. This
522 situation implies that the possible fluctuations of tracer gas concentration in the considered locations,
523 as the tracer gas concentration peaks occurrence, are not completely registered. Experimental time
524 periods are adjusted to assess this situation following the criterion included as Supplementary
525 Information, however a higher frequency tracer gas concentration probes could enrich the gathered
526 information about the recurrent perturbation registered in tracer gas concentration. The use of a

527 equipment that allows performing a higher measurement frequency could lead to a better
528 understanding of the peaks occurrence.

529

530 **5 Conclusions**

531 Experimental tests have been carried out to determine ventilation performance and contaminant
532 exposure in a representative case of study of a typical individual hospital room configuration using
533 two different mixing ventilation systems and three air ventilation rates and connected with previous
534 DV studies. In view of the results of each test and the comparisons between them, the following
535 conclusions can be stated:

- 536 • Airflow patterns generated by G and S ventilation configurations influence ventilation
537 efficiency (ε^a , ε_p^c and ε_p^a) and contaminant exposure (e_p^c and IF) of HW. Swirl diffusers (S)
538 generate a better mixing ventilation situation, leading to a better performance and exposure
539 indices. So S supply could be considered as a more reliable strategy in hospital rooms. It has
540 also been noted that HW exposure results are better if S supply is combined with D exhaust.
- 541 • Air renovation (ACH) has a very low influence in the HW exposure for S supply cases.
542 However, the change of ACH for G supply cases determine completely different behavior of
543 the dispersion of exhaled contaminants. For GU a short circuit between the inlet and the
544 exhaust is generated for 9ACH producing the highest exposure values in the inhalation of
545 HW. For GD using 6 and 9 ACH the lack of a perfect mixing of the air in the room generates
546 high peak values of exposure in the inhalation of HW.
- 547 • Being the human exhalation a transient process, the exposure to exhaled contaminants is also
548 observed as a transient process. This fact leads to average (e_p^c) and peak ($e_{p,125\%}^c$ and $e_{p,max}^c$)
549 different exposure values depending on the experimental case. Low average exposure (e_p^c)

550 cases may present punctual high peak exposure ($e_{P,max}^c$) values. The peak frequency
551 ($f_{P,125\%}$), which is lower for S cases, can increase with the air ventilation rate .

552 • The exposure to contaminants of HW is lower when displacement ventilation strategy is used
553 instead of mixing ventilation strategy. A similar exposure to contaminants is obtained in DV
554 and MV systems when 12 ACH is used.

555 Considering all the results, it has been found that using a mixing ventilation strategy if a perfect
556 mixing is not reached the ACH and the relative positions between supply and exhaust locations
557 determine the HW exposure. The transient nature observed of the dispersion of the exhaled
558 contaminants makes the authors think of the necessity of study the exposure using high frequency
559 contaminant sensors. A deeper study considering different relative positions between the people
560 occupying the room and the supply/exhaust positions will add knowledge about contaminants
561 exposure in indoor environments.

562 **6 Acknowledgements**

563 The authors acknowledge the financial support received from the Ministerio de Economía y
564 Competitividad, Secretaría de Estado de Investigación, Desarrollo e Innovación, Spain, to the
565 National R&D project TRACER with reference DPI2014-55357-C2-2-R, entitled “Ventilation
566 system influence on airborne transmission of human exhaled bioaerosols. Cross infection risk
567 evaluation”. This project is cofinanced by the European Regional Development Fund (ERDF).

568 **7 References**

- 569 [1] C.B. Beggs, L.D. Knibbs, G.R. Johnson, L. Morawska, Environmental contamination and
570 hospital-acquired infection: factors that are easily overlooked, *Indoor Air*. 25 (2015) 462–474.
571 doi:10.1111/ina.12170.
- 572 [2] M.P. Atkinson, L.M. Wein, Quantifying the routes of transmission for pandemic influenza,
573 *Bull. Math. Biol.* 70 (2008) 820–867. doi:10.1007/s11538-007-9281-2.
- 574 [3] J.W. Tang, Investigating the airborne transmission pathway - different approaches with the
575 same objectives, *Indoor Air*. 25 (2015) 119–124. doi:10.1111/ina.12175.
- 576 [4] I. Eames, J.W. Tang, Y. Li, P. Wilson, Airborne transmission of disease in hospitals., J. R.

- 577 Soc. Interface. 6 Suppl 6 (2009) S697–S702. doi:10.1098/rsif.2009.0407.focus.
- 578 [5] Centers for Disease Control and Prevention, Guidelines for preventing the transmission of
579 Mycobacterium tuberculosis in health-care facilities., MMWR Morb Mortal Wkly Rep. 43
580 (1994) 1–132. doi:10.2307/42000931.
- 581 [6] F.A. Berlanga, I. Olmedo, M. Ruiz de Adana, Experimental analysis of the air velocity and
582 contaminant dispersion of human exhalation flows, Indoor Air. (2016) 1–13.
583 doi:10.1111/ina.12357.
- 584 [7] J.W. Tang, A. Nicolle, C. Klettner, J. Pantelic, L. Wang, A. Suhaimi, et al., Airflow dynamics
585 of human jets: sneezing and breathing - potential sources of infectious aerosols, PLoS One. 8
586 (2013) e59970. doi:10.1371/journal.pone.0059970.
- 587 [8] J.K. Gupta, C.H. Lin, Q. Chen, Flow dynamics and characterization of a cough, Indoor Air. 19
588 (2009) 517–525. doi:10.1111/j.1600-0668.2009.00619.x.
- 589 [9] C.Y.H. Chao, M.P. Wan, L. Morawska, G.R. Johnson, Z.D. Ristovski, M. Hargreaves, et al.,
590 Characterization of expiration air jets and droplet size distributions immediately at the mouth
591 opening, J. Aerosol Sci. 40 (2009) 122–133. doi:10.1016/j.jaerosci.2008.10.003.
- 592 [10] X. Xie, Y. Li, A.T.Y. Chwang, P.L. Ho, W.H. Seto, How far droplets can move in indoor
593 environments - revisiting the Wells evaporation-falling curve, Indoor Air. 17 (2007) 211–225.
594 doi:10.1111/j.1600-0668.2007.00469.x.
- 595 [11] W.F. Wells, On air-borne infection. II. Droplets and droplet nuclei, Am. J. Hyg. 20 (1934)
596 611–618.
- 597 [12] A. Jurelionis, L. Gagytė, T. Prasauskas, D. Čiužas, E. Krugly, L. Šėduikytė, et al., The impact
598 of the air distribution method in ventilated rooms on the aerosol particle dispersion and
599 removal: The experimental approach, Energy Build. 86 (2015) 305–313.
600 doi:http://dx.doi.org/10.1016/j.enbuild.2014.10.014.
- 601 [13] L. Liu, Y. Li, P. V. Nielsen, J. Wei, R.L. Jensen, Short-range airborne transmission of
602 expiratory droplets between two people, Indoor Air. (2016) 1–11. doi:10.1111/ina.12314.
- 603 [14] M. Bivolarova, W. Kierat, E. Zavrl, Z. Popiolek, A. Melikov, Effect of airflow interaction in
604 the breathing zone on exposure to bio-effluents, Build. Environ. 125 (2017) 216–226.
605 doi:10.1016/j.buildenv.2017.08.043.
- 606 [15] A. Jurelionis, L. Gagyte, L. Seduikyte, T. Prasauskas, D. Ciuzas, D. Martuzevičius, Combined
607 air heating and ventilation increases risk of personal exposure to airborne pollutants released
608 at the floor level, Energy Build. 116 (2016) 263–273. doi:10.1016/j.enbuild.2016.01.011.
- 609 [16] Y. Lv, H. Wang, S. Wei, The transmission characteristics of indoor particles under two
610 ventilation modes, Energy Build. 163 (2018) 1–9. doi:10.1016/j.enbuild.2017.12.028.
- 611 [17] A.K. Melikov, Z.D. Bolashikov, E. Georgiev, Novel ventilation strategy for reducing the risk
612 of airborne cross infection in hospital rooms, (2011) 1–6.
- 613 [18] N.J. Adams, D.L. Johnson, R. a. Lynch, The effect of pressure differential and care provider
614 movement on airborne infectious isolation room containment effectiveness, Am. J. Infect.
615 Control. 39 (2011) 91–97. doi:10.1016/j.ajic.2010.05.025.
- 616 [19] J.D. Siegel, E. Rhinehart, M. Jackson, L. Chiarello, 2007 Guideline for Isolation Precautions:
617 Preventing Transmission of Infectious Agents in Health Care Settings, Am. J. Infect. Control.
618 35 (2007). doi:10.1016/j.ajic.2007.10.007.
- 619 [20] E. Lingaas, J.P. Rydock, Best practice in design and testing of isolation rooms in Nordic
620 hospitals, Round Table Ser. - R. Soc. Med. (2007) 87–107.
- 621 [21] Victorian Advisory Committee on Infection Control, Guidelines for the classification and
622 design of isolation rooms in health care facilities, 1st ed., Victorian Government, Melbourne,
623 2007.
- 624 [22] L. Sehulster, R.Y.W. Chinn, Guidelines for environmental infection control in health-care
625 facilities, Morb. Mortal. Wkly. Rep. 52 (2003) 1–42.
- 626 [23] F. Memarzadeh, W. Xu, Role of air changes per hour (ACH) in possible transmission of

- 627 airborne infections, *Build. Simul.* 5 (2012) 15–28. doi:10.1007/s12273-011-0053-4.
- 628 [24] P. Kalliomäki, P. Saarinen, J.W. Tang, H. Koskela, Airflow patterns through single hinged
629 and sliding doors in hospital isolation rooms - Effect of ventilation, flow differential and
630 passage, *Build. Environ.* 107 (2016) 154–168. doi:10.1016/j.buildenv.2016.07.009.
- 631 [25] P. Kumar, C. Martani, L. Morawska, L. Norford, R. Choudhary, M. Bell, et al., Indoor air
632 quality and energy management through real-time sensing in commercial buildings, *Energy*
633 *Build.* 111 (2016) 145–153. doi:10.1016/j.enbuild.2015.11.037.
- 634 [26] W. Yu, B. Li, H. Jia, M. Zhang, D. Wang, Application of multi-objective genetic algorithm to
635 optimize energy efficiency and thermal comfort in building design, *Energy Build.* 88 (2015)
636 135–143. doi:10.1016/j.enbuild.2014.11.063.
- 637 [27] A. Kabanshi, H. Wigö, M. Sandberg, Experimental evaluation of an intermittent air supply
638 system - Part 1: Thermal comfort and ventilation efficiency measurements, *Build. Environ.* 95
639 (2016) 240–250. doi:10.1016/j.buildenv.2015.09.025.
- 640 [28] H. Qian, Y. Li, P. V. Nielsen, C.E. Hyldgaard, T.W. Wong, a T.Y. Chwang, Dispersion of
641 exhaled droplet nuclei in a two-bed hospital ward with three different ventilation systems,
642 *Indoor Air.* 16 (2006) 111–28. doi:10.1111/j.1600-0668.2005.00407.x.
- 643 [29] Y. Yin, W. Xu, J.K. Gupta, A. Guity, P. Marmion, A. Manning, et al., Experimental Study on
644 Displacement and Mixing Ventilation Systems for a Patient Ward, *HVAC&R Res.* 15 (2009)
645 1175–1191. doi:10.1080/10789669.2009.10390885.
- 646 [30] P. V. Nielsen, C.E. Hyldgaard, A.K. Melikov, H. Andersen, M. Soennichsen, Personal
647 exposure between people in a room ventilated by textile terminals—with and without
648 personalized ventilation, *HVAC R Res.* 13 (2007) 635–643.
649 doi:10.1080/10789669.2007.10390976.
- 650 [31] J.W. Tang, C.J. Noakes, P. V. Nielsen, I. Eames, A. Nicolle, Y. Li, et al., Observing and
651 quantifying airflows in the infection control of aerosol- and airborne-transmitted diseases: An
652 overview of approaches, *J. Hosp. Infect.* 77 (2011) 213–222. doi:10.1016/j.jhin.2010.09.037.
- 653 [32] M. Bivolarova, A.K. Melikov, C. Mizutani, K. Kajiwara, Z.D. Bolashikov, Bed-integrated
654 local exhaust ventilation system combined with local air cleaning for improved IAQ in
655 hospital patient rooms, *Build. Environ.* 100 (2016) 10–18.
656 doi:10.1016/j.buildenv.2016.02.006.
- 657 [33] M. Hyttinen, A. Rautio, P. Pasanen, T. Reponen, G.S. Earnest, A. Streifel, et al., Airborne
658 Infection Isolation Rooms - A Review of Experimental Studies, *Indoor Built Environ.* 20
659 (2011) 584–594. doi:10.1177/1420326X11409452.
- 660 [34] G. Cao, H. Awbi, R. Yao, Y. Fan, K. Sirén, R. Kosonen, et al., A review of the performance
661 of different ventilation and airflow distribution systems in buildings, *Build. Environ.* 73
662 (2014) 171–186. doi:10.1016/j.buildenv.2013.12.009.
- 663 [35] Y.C. Tung, S.C. Hu, T.I. Tsai, I.L. Chang, An experimental study on ventilation efficiency of
664 isolation room, *Build. Environ.* 44 (2009) 271–279. doi:10.1016/j.buildenv.2008.03.003.
- 665 [36] J.M. Villafruela, F. Castro, J.F. San Jose, J. Saint-Martin, Comparison of air change
666 efficiency, contaminant removal effectiveness and infection risk as IAQ indices in isolation
667 rooms, *Energy Build.* 57 (2013) 210–219. doi:10.1016/j.enbuild.2012.10.053.
- 668 [37] F.A. Berlanga, M.R. de Adana, I. Olmedo, J.M. Villafruela, J.F. San José, F. Castro, et al.,
669 Experimental evaluation of thermal comfort, ventilation performance indices and exposure to
670 airborne contaminant in an Airborne Infection Isolation Room equipped with a displacement
671 air distribution system, *Energy Build.* (2017). doi:10.1016/J.ENBUILD.2017.09.100.
- 672 [38] H. Qian, Y. Li, P. V. Nielsen, C.E. Hyldgaard, Dispersion of exhalation pollutants in a two-
673 bed hospital ward with a downward ventilation system, *Build. Environ.* 43 (2008) 344–354.
674 doi:10.1016/j.buildenv.2006.03.025.
- 675 [39] M.P. Wan, C.Y.H. Chao, Y.D. Ng, G.N. Sze To, W.C. Yu, Dispersion of expiratory droplets
676 in a general hospital ward with ceiling mixing type mechanical ventilation system, *Aerosol*

- 677 Sci. Technol. 41 (2007) 244–258. doi:10.1080/02786820601146985.
- 678 [40] E. Mundt, H.M. Mathisen, P. V. Nielsen, A. Moser, Ventilation Effectiveness, 2004.
- 679 [41] J.W. Tang, Y. Li, I. Eames, P.K.S. Chan, G.L. Ridgway, Factors involved in the aerosol
680 transmission of infection and control of ventilation in healthcare premises, *J. Hosp. Infect.* 64
681 (2006) 100–114. doi:10.1016/j.jhin.2006.05.022.
- 682 [42] F.A. Berlanga, M. Ruiz de Adana, I. Olmedo, Diseño y construcción de maniqués térmicos
683 para la realización de ensayos experimentales de sistemas de climatización, in: *Proc. IX*
684 *Congr. Nac. Ing. Termodinámica, Cartagena, 2015*: pp. 1–8. doi:978-84-606-8931-7.
- 685 [43] Technical Comitee for Ergonomics of the physical environment, ISO 7726 Ergonomics of the
686 thermal envinonment - Instruments for measuring physical quantities, 2nd ed., ISO, 1998.
- 687 [44] R. Tomasi, M. Krajčik, A. Simone, B.W. Olesen, Experimental evaluation of air distribution
688 in mechanically ventilated residential rooms: Thermal comfort and ventilation effectiveness,
689 *Energy Build.* 60 (2013) 28–37. doi:10.1016/j.enbuild.2013.01.003.
- 690 [45] M. Krajčik, A. Simone, B.W. Olesen, Air distribution and ventilation effectiveness in an
691 occupied room heated by warm air, *Energy Build.* 55 (2012) 94–101.
692 doi:10.1016/j.enbuild.2012.08.015.
- 693 [46] ISO - AEN/CTN 81, ISO 7730. Ergonomics of the thermal environment—Analytical
694 determination and interpretation of thermal comfort using calculation of the PMV and PPD
695 indices and local thermal comfort criteria, ISO, Geneva, 2005.
- 696 [47] ASHRAE, F09 SI: Thermal Comfort, in: *ASHRAE Handb. Fundam.*, 2009: p. 9.1-9.30.
- 697 [48] J. Laverge, M. Spilak, A. Novoselac, Experimental assessment of the inhalation zone of
698 standing, sitting and sleeping persons, *Build. Environ.* 82 (2014) 258–266.
699 doi:10.1016/j.buildenv.2014.08.014.
- 700 [49] M. De Carli, B.W. Olesen, Field measurements of operative temperatures in buildings heated
701 or cooled by embedded water-based radiant systems, in: *ASHRAE Trans.*, 2002: pp. 714–725.
- 702 [50] Z.D. Bolashikov, A.K. Melikov, W. Kierat, Z. Popioek, M. Brand, Exposure of health care
703 workers and occupants to coughed airborne pathogens in a double-bed hospital patient room
704 with overhead mixing ventilation, in: *HVAC R Res.*, 2012: pp. 602–615.
705 doi:10.1080/10789669.2012.682692.
- 706 [51] J. Pantelic, K.W. Tham, Adequacy of air change rate as the sole indicator of an air distribution
707 system’s effectiveness to mitigate airborne infectious disease transmission caused by a cough
708 release in the room with overhead mixing ventilation: A case study, *HVAC R Res.* 19 (2013)
709 947–961. doi:10.1080/10789669.2013.842447.
- 710 [52] A.K. Melikov, Z.D. Bolashikov, W. Kierat, Z. Popiolek, Does increased ventilation help
711 reduce cross-infection in isolation hospital wards?, in: *Proc. CLIMA 2010, Antalya, 2010*.
- 712 [53] I. Olmedo, P. V. Nielsen, M. Ruiz de Adana, R.L. Jensen, P. Grzelecki, Distribution of
713 exhaled contaminants and personal exposure in a room using three different air distribution
714 strategies., *Indoor Air.* 22 (2012) 64–76. doi:10.1111/j.1600-0668.2011.00736.x.
- 715